View Article Online / Journal Homepage / Table of Contents for this issue
Dynamic Article Links

CrystEngComm

Cite this: *CrystEngComm*, 2011, **13**, 5354

www.rsc.org/crystengcomm

PAPER

Structural systematics and conformational analyses of a 3 × 3 isomer grid of nine *N*-(tolyl)pyridinecarboxamides and three chlorinated relatives†

Pavle Mocilac and John F. Gallagher*

Received 4th February 2011, Accepted 30th March 2011
DOI: 10.1039/c1ce05169e

A 3 × 3 isomer grid of nine *N*-(tolyl)pyridinecarboxamides (**NxxM**, x = *para-*/*meta-*/*ortho-*) integrating crystal structure analyses, *ab initio* calculations (*gas phase* and PCM-SMD solvated in CH_2Cl_2, H_2O) and conformational studies is described. Three 5-Cl-**NoxM** derivatives (side-products from the **NoxM** syntheses) and **NmpFM** (a 50 : 50 mixture of **NmpF** and **NmpM**) are reported. The six **NpxM**/**NmxM** isomers aggregate *via* N–H···N or N–H···O=C hydrogen bonds, whereas the six **NoxM**/5-Cl-**NoxM** structures exhibit intramolecular N–H···N interactions influencing co-planarity. The **NmmM** isomer is isomorphous and isostructural with its *bridge-flipped* **Mmm** isomer providing a rare case of *isostructuralism* between such isomers. Our objectives are to (a) understand correlations between the *p-*/*m-*/*o-***N**/CH_3 substituent permutations with solid state molecular conformations and supramolecular aggregation, (b) explain the influence of molecular conformation on inter/intramolecular interactions, (c) correlate physico-chemical properties and (d) compare and rationalise differences between crystal and calculated structures.

1. Introduction

Advances in chemical informatics and machine-learning methods are being exploited in the *on-going* screening and prioritisation of promising lead molecules in drug design.[1–4] The wealth of information from millions of accessible chemical compounds demands effective methods of data collation and analysis. The impetus is driven by the current cost of developing a new drug which is estimated to be in excess of 1 billion US$.

In tandem, comprehensive structural studies of small *drug-like* molecules have been principally facilitated by technological advancements in solid state analytical techniques and methods,[5,6] while computational approaches with molecular structure prediction have seen a dramatic increase in the ability to study larger numbers of structures to higher levels of theory.[7] Structural systematic studies rely on merging several areas of structural research and the ability to collate, integrate and correlate physico-chemical data to provide an insight into physical or chemical properties within, or between, molecular organic groups.[5,6,8,9]

Our current research is directed towards integrating crystal structure analyses with computational (*ab initio*) modelling methods and exploring the influence and positional influence of different functional groups *e.g.* N/F/Cl/Br/I atoms, Me/OMe groups in semi-rigid *drug-like* molecules on inter- and intramolecular interactions, conformations and solid-state packing. The 3 × 3 isomer grids of structurally similar aromatic amides *i.e.* methyl-*N*-(pyridyl)benzamides (**Mxx**)[10] and *N*-(fluorophenyl) pyridinecarboxamides (**NxxF**)[11] are present as scaffolds in many important benzamide and picolinamide drugs. Herein, a series of nine *N*-(tolyl)pyridinecarboxamides (**NxxM**, x = *para-*/*meta-*/*ortho-*, Scheme 1a) and three *N*-(tolyl)(5-chloropyridine)carboxamides as 5-Cl-**NoxM** (Scheme 1b) is described. The **NxxM** grid (related to nicotinamides)[12] is similar to our **NxxF** isomer grid,[11] with the F atom replaced by a methyl group and differs from **Mxx** by a reversed amide bridge (or *bridge-flip*).[13,14] Related series of *bridge-flipped* isomers have been analysed by Ojala and co-workers to compare and contrast intermolecular interactions in *bridge-flipped* isomers.[13,14]

The **Mxx** isomers are 4-aminopyridine (4-AP) derivatives and the **NxxM** series are (as for **NxxF**) the reverse or indirect *pseudo*-derivatives of 4-AP. Such 4-AP derivatives have potential neuropharmacological behaviour as K^+ channel modulators[15,16] and few studies are available for most **NxxM** isomers (apart from **NopM**). The **NppM** isomer has been examined as a ligand in metal complexes and complex-based polymers with Cu,[17,18] whereas **NoxM** ligands have been widely studied in metal complexes *e.g.* Fe,[19] Ni,[19] Co,[19,20] Ru,[21,22] Ir,[23] Au,[24] Mn[25,26] and Pt[27] with potential and defined catalytic or electrochemical properties.

Our objectives are to study the **NxxM** series using both experimental and *in silico* methods. Comparisons involve

School of Chemical Sciences, Dublin City University, Dublin, 9, Ireland. E-mail: john.gallagher@dcu.ie; Web: http://doras.dcu.ie; Fax: +353-1-7005503; Tel: +353-1-7005114

† Electronic supplementary information (ESI) available: The ^1H, ^{13}C NMR and spectroscopic data for all nine **NxxM**, **NmpFM** and three 5-Cl-**NoxM** isomers with listings of the *ab initio* calculations. CCDC reference numbers 809618–809630. For ESI and crystallographic data in CIF or other electronic format see DOI: 10.1039/c1ce05169e

This journal is © The Royal Society of Chemistry 2011

Published on 28 April 2011. Downloaded by University of Birmingham on 30/10/2014 11:07:57.

View Article Online

Published on 28 April 2011. Downloaded by University of Birmingham on 30/10/2014 11:07:57.

a)

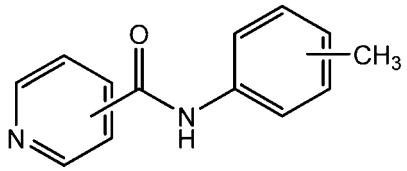

	para-tolyl	*meta*-tolyl	*ortho*-tolyl
para (4-pyridinoyl)	**NppM**	**NpmM**	**NpoM**
meta (3-pyridinoyl)	**NmpM**	**NmmM**	**NmoM**
ortho (2-pyridinoyl)	**NopM**	**NomM**	**NooM**

b)

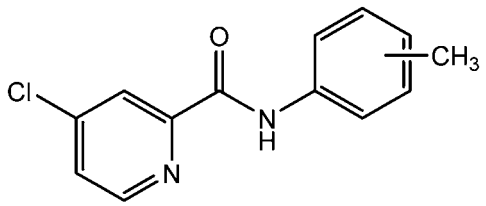

	para-tolyl	*meta*-tolyl	*ortho*-tolyl
ortho (5-chloro-2-pyridinoyl)	5-Cl-**NopM**	5-Cl-**NomM**	5-Cl-**NooM**

Scheme 1 (a) Structures and nomenclature of the nine **NxxM** isomers. (b) Structures and nomenclature of three 5-Cl-**NxxM** isomers.

analysis of the (a) synthesis and characterisation data (b) crystal structures, (c) computational calculations (geometry optimisation in the *gas phase* and solvated forms CH_2Cl_2 and H_2O), molecular energies and ΔG_{solv} and (d) conformational analyses of the optimised structures.

The questions to be addressed involve correlations between the various permutations of the **N**/CH_3 group site with molecular conformation, solid-state aggregation and physicochemical properties. The formation of inter/intramolecular hydrogen bonds in the solid state and their influences on molecular conformations are analysed and collated with conformational and structural differences between both theory and experiment. Comparisons with the **Mxx** and **NxxF** isomer grids[10,11] together with spectroscopic data and crystal structures of three 5-Cl-**NoxM** side-products are detailed, together with an *unusual* mixed **NmpF** : **NmpM** system as **NmpFM** (having equal **F**/$\mathbf{CH_3}$ components).

2. Experimental section

2.1. Materials and equipment

The analytical and spectroscopic equipment, spectroscopic and computational methods used in this research are as reported previously[10,11] with two exceptions: the solid state IR spectroscopy was performed using the attenuated total reflection (ATR) method on a Perkin-Elmer Spectrum 100 FT-IR Spectrometer; and single crystal studies were undertaken on an Oxford Diffraction Gemini-S Ultra diffractometer using Mo-radiation at room temperature [294(1) K].

2.2. General description of NxxM and 5-Cl-NoxM synthesis

The **NxxM** series was synthesised using standard nucleophilic acyl substitution reactions (Schotten–Baumann reaction) between *p*-/*m*-/*o*-toluidines and *p*-/*m*-/*o*-pyridinoyl chloride hydrochlorides in the presence of one equivalent of triethylamine (Et_3N) as base and CH_2Cl_2 as solvent. Detailed descriptions of the synthetic and purification procedures are provided in the ESI† (Section 1).

Generally, the yields (30–70%) and purity were modest to excellent with the exception of the **NoxM** triad, as the picolinoyl chloride starting material contains a small quantity of 5-chloropicolinoyl chloride. This impurity is an inevitable by-product of the original 2-pyridinoyl chloride synthesis using $SOCl_2$. Flash column chromatography (as described in the ESI†) was successfully employed in the purification of the **NoxM** triad, separating each **NoxM** from the 5-Cl-**NoxM** contaminant. The three 5-Cl-**NoxM** compounds were isolated in low yield and characterised by both spectroscopic methods and single crystal X-ray diffraction. In addition, the structure of **NmpFM** (isolated from a 50 : 50 mixture of **NmpF** and **NmpM**) is compared with both **NmpF**[11] and **NmpM**.

2.3. Single crystal growth and X-ray crystallography methods

All nine **NxxM** crystal samples and three 5-Cl-**NoxM** single crystals were obtained by slow evaporation at 4 °C, typically from either $CHCl_3$ or ethyl acetate. However, for **NomM**, suitable single crystals were grown from cyclohexane and for **NooM**, crystals were eventually grown from methanol after many crystallization attempts from several solvents under a wide range of crystallization conditions.

Single crystal X-ray data for all nine **NxxM** isomers, the three 5-Cl-**NoxM** and **NmpFM** were collected on an Oxford Diffraction Gemini-S Ultra diffractometer at 294(1) K, with θ range 2–25° minimum and 100% data coverage to 25° (on θ).[28] Data reduction procedures and absorption corrections are standard;[28] comprehensive details have been published elsewhere.[10,11] All structures were solved using the SHELXS97[29] direct methods program and refined by full matrix least squares calculations on F^2 with all non-hydrogen atoms having anisotropic displacement parameters. Hydrogen atoms were treated as riding atoms using the SHELXL97 defaults at 294(1) K except for the amide N–H (isotropic refinement) using the OSCAIL software.[30] Selected crystallographic and structural information are detailed in Tables 1 and 2 and the ESI† (the amide as a five atom plane). Molecular and hydrogen bonding diagrams (Fig. 1–12) were

Table 1 Selected crystallographic data for **NxxM**, **NmpFM**, and 5-Cl-**NoxM**

Structure	Space group	Z'	Volume	R-Factors
NppM	$P2/c$	1	1089.98(9)	0.051, 0.141
NpmM	$P2_1/n$	1	1133.67(6)	0.034, 0.083
NpoM	Cc	1	1123.84(11)	0.030, 0.081
NmpM	$P2_1/c$	1	1074.47(8)	0.036, 0.073
NmmM	$P\bar{1}$	2	1085.36(7)	0.057, 0.179
NmoM	$Pbca$	1	2239.48(10)	0.040, 0.107
NopM	$P2_1/c$	1	1100.40(7)	0.035, 0.083
NomM	$P2_1$	2	1178.92(8)	0.029, 0.045
NooM	$P2_1/c$	1	1099.41(5)	0.037, 0.093
NmpFM	$Pna2_1$	0.5 : 0.5	1062.66(18)	0.035, 0.093
5-Cl-**NopM**	$Pca2_1$	1	1189.24(3)	0.026, 0.065
5-Cl-**NomM**	$P2_1/c$	1	1204.0(5)	0.066, 0.233
5-Cl-**NooM**	$P2_1/n$	1	1171.93(15)	0.038, 0.103

View Article Online

Published on 28 April 2011. Downloaded by University of Birmingham on 30/10/2014 11:07:57.

Table 2 Salient structural features of **NxxM**, **NmpFM** and 5-Cl-**NoxM**

Structure	C_6/C_5N	C_6/amide[a]	C_5N/amide[a]	N···N/O	Packing[b]
NppM	66.45(3)	34.96(5)	31.54(5)	**3.0529(14)**	1D chains
NpmM	4.50(10)	14.73(7)	19.19(7)	*3.1265(18)*	2D sheets
NpoM	83.90(6)	68.04(7)	28.26(9)	**2.825(2)**	1D chains
NmpM	4.11(9)	4.11(9)	1.06(9)	*3.223(2)*	1D catemers
NmmM	57.23(6) 64.31(6)	24.69(6) 36.68(6)	33.93(8) 28.23(8)	*3.090(2)*, *3.078(2)*	1D chains
NmoM	89.99(5)	60.63(5)	29.55(6)	**2.8978(15)**	1D chains
NopM	33.63(4)	29.45(5)	4.33(4)	*2.6548(18)*	1D chain
NomM[c]	14.61(14) 9.71(17)	15.39(14) 6.54(15)	4.63(15) 16.03(16)	**3.241(3)**,[c] **3.132(3)**, *2.683(4)*, *2.703(4)*	2D sheets
NooM	1.91(5)	1.47(5)	1.70(5)	*2.6209(15)*	Dimers
NmpFM	5.00(14)	3.21(13)	1.93(13)	*3.207(2)*	2D Cat sheets
5-Cl-**NopM**	26.42(2)	22.25(2)	4.20(3)	*2.6514(9)*	2D sheet
5-Cl-**NomM**[c]	4.35(13)	8.98(12)	12.79(12)	**3.035(4)**,[c] *2.683(4)*	1D chains
5-Cl-**NooM**	2.30(5)	4.38(6)	2.80(5)	*2.6690(15)*	1D tape

[a] Amide plane calculated as a five atom plane *i.e.* $_{Ar}C–C(=O)N–C_{Ar}$. [b] Packing is noted as *primary packing* unless for competing strengths and for both **NoxM** and 5-Cl-**NoxM**, additional interactions are considered where the primary interaction is intramolecular $N–H\cdots N_{pyridine}$. [c] For **NomM** and 5-Cl-**NomM** both intramolecular $N–H\cdots N$ and intermolecular **N–H···O=C** interactions are quoted.

generated using PLATON.[31] All searches and analyses of the Cambridge Structural Database (CSD) were performed with the November 2010 release (version 5.32).[5,32]

2.4. Computational methods

The computational methods and procedures used are identical to our previous studies.[10,11] The *ab initio* DFT geometry optimisation (B3LYP/6-311++G) of the nine compound **NxxM** isomer grid was performed using Gaussian03/09[33] both in the *gas phase* and with two solvents, CH_2Cl_2 and H_2O (PCM-SMD solvation model).[34] High accuracy energy calculations including ΔG_{solv} were obtained with the CBS-QB3[35] compound method with results provided in the ESI† (Section 5.1).

Our objective is comparison of the **NxxM** optimised structures/conformations with each **NxxM** crystal structure conformation. Analysis was undertaken using PES scans of the two key dihedral angles over a range ±180° both in *gas phase* and solvents, as the C26–C21–C1=O1 dihedral (α, **N**-ring) and C1–N1–C11–C12 dihedral (β, **M**-ring). Each asymmetric (*meta*- or *ortho*-) ring can adopt (relative to the amide linker) two conformations (either *syn* or *anti*) (Scheme 2). The pyridine (**N**) or tolyl (**M**) rings can be either ***syn*** (**N-*syn***, **M-*syn***) or ***anti*** (**N-*anti***, **M-*anti***) and this does not apply for *para*-substitution.

The results provide PES diagrams showing the conformational preferences either as (***syn*/*anti***) and the rotational barriers in kJ mol^{-1}. Moreover, the resulting conformational analysis is an important tool for the validation of the optimised structures.

3. Results and discussion

3.1. Comment on general characteristics and synthesis

All **NxxM** compounds are white, odourless solids, soluble in various organic solvents (MeOH, ethyl acetate, CH_2Cl_2, $CHCl_3$, 2-propanol, DMSO), poorly soluble in cyclohexane, hexane, toluene and insoluble in water. The overall yields were moderate to good and the **NxxM** and 5-Cl-**NxxM** compound purity was excellent after column chromatography.

The **NpxM**, **NmxM** and **NopM** isomers crystallize easily from a range of solvents. However, after purification by column chromatography **NomM** proved reluctant to crystallise from several solvents using different crystallization conditions. Crystals were finally obtained using stress cooling with liquid N_2 followed by recrystallization from cyclohexane. Solid **NomM** differs from the other **NxxM** isomers and looks ceraceous rather than crystalline. **NooM** crystals were obtained after several trials from CH_3OH.

In general, melting points decrease consecutively from the symmetrical **NppM** to the unsymmetrical **NomM**. The lowest melting point for **NomM** (~50 °C) is unusual, suggesting, together with other macroscopic characteristics, weak and unusual intermolecular interactions in the **NomM** crystal structure (see Sections 3.3.4.2 and 3.4 below).

3.2. Comment on spectroscopic data

All spectroscopic data, including ^1H and ^{13}C NMR as well as IR spectra, are given in the ESI† (Section 2). The NMR data (^1H, ^{13}C) show a high level of modularity within the pyridine and tolyl rings across the **NxxM** isomer grid as expected. As for the **NxxF** series[11] the spectroscopic data reveal the presence of the intramolecular N–H–N_{pyr} interactions in the **NoxM** and 5-Cl-**NoxM** triads. The chemical shifts for the amide hydrogen (N–H) in the six **NpxM/NmxM** isomers in $CDCl_3$ are *ca.* 8.0 ppm, while in DMSO-d^6 are shifted to *ca.* 10.3 ppm from interacting with the S=O group. In the **NoxM** triad the chemical shifts are ~10.0 ppm (in $CDCl_3$) and 10.5 ppm (in DMSO-d^6) indicating the presence of additional internal

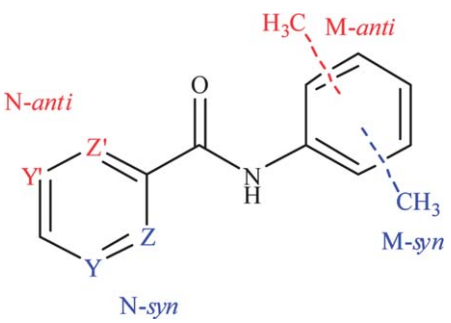

Scheme 2 Possible conformations of the **NxxM** isomers.

 This journal is © The Royal Society of Chemistry 2011

View Article Online

Published on 28 April 2011. Downloaded by University of Birmingham on 30/10/2014 11:07:57.

deshielding of the amide hydrogen as a result of interacting with the neighbouring N_{pyr} atom. The intramolecular N1–H1···N22 interaction in the **NoxM** triad is also noted in the ATR-IR with one sharp N–H stretching band at 3336 (**NopM**), 3286 (**NomM**), 3343 cm^{-1} (**NooM**) in contrast with weaker, more diffuse N–H vibrations in the **NpxM**/**NmxM** series (see below).

3.3 Crystallographic data and analysis

3.3.1 General comments. The nine **NxxM** and three 5-Cl-**NoxM** crystal structures crystallise in seven common space groups with only CH_3 methyl group rotational disorder of the H atom sites in six of the twelve structures (treated with AFIX 127). Seven **NxxM** and three 5-Cl-**NoxM** isomers crystallise with $Z' = 1$ and **NmmM**, **NomM** with $Z' = 2$ (Table 1). The twelve compounds can be classified into two distinct (**NpxM**, **NmxM**) and (**NoxM**, 5-Cl-**NoxM**) groups.

The distinct intermolecular feature of the **NxxM** crystal structures is aggregation in the solid state either *via* $_{amide}$N–H···$N_{pyridine}$ or N–H···O=C hydrogen bonds, and usually in different space groups. The primary hydrogen bond in **NpmM**, **NmpM** and **NmmM** is $_{amide}$N–H···$N_{pyridine}$ usually in tandem with a much weaker C–H···O=C interaction (*ca.* 0.2 Å longer). In **NppM**, **NpoM** and **NmoM**, the primary interaction is $_{amide}$N–H···O=C_{amide} with additional weak contacts (*ca.* 2.70 Å for C–H···N) involving the pyridine–N atom and pyridine ring. In the related **NxxF** series, only **NppF**[11] has amide···amide interactions as the primary interaction [as typical C(4) chains] and with no additional longer C–H···N interactions.

In the three **NoxM** crystal structures, the intramolecular N–H···N interaction dominates with additional longer C–H···O interactions in **NopM** (+2) and **NooM** (+1), but in **NomM** an additional N–H···O=C interaction (H···O = 2.32(3), 2.41(2) Å) with C–H···O=C forms a hydrogen bonded $R_2^1(6)$ ring (Fig. 8). The **NomM** crystals provide the poorest quality structure with a high R_{int} [0.096] and unexpected aggregation; **NomM** has the lowest melting point range of 49–50 °C. Three 5-Cl-**NoxM** structures also display the intramolecular N1–H1···N22 interaction and are similar to **NoxM** except for 5-Cl-**NomM** with N–H···O=C/π···π stacking interactions being atypical of either the **NoxM** or **NoxF**[11] structures. In addition, the mixed fluoro/CH_3 system (**NmpFM**) is isolated from a 50 : 50 mixture of **NmpF**/**NmpM** and is compared with the tetrameric assembly in **NmpF**[11] and catemeric **NmpM** structure.

As noted above, the primary hydrogen bonding in the **NxxM** isomers can be classed into three groups, each with distinctive IR spectra in the N–H stretch region between 3600 cm^{-1} and 2800 cm^{-1}. The **NpmM**, **NmpM** and **NmmM** isomers with $_{amide}$N–H···$N_{pyridine}$ as the main intermolecular interaction exhibit two principal N–H stretch vibrations at 3274 cm^{-1} and 3066 cm^{-1} with several smaller peaks. The second group comprising **NppM**, **NpoM** and **NmoM** with $_{amide}$N–H···O=C_{amide} interactions has a smaller band at 3073 cm^{-1} and one close to 3322 cm^{-1} (3237 cm^{-1} for **NpoM** and **NmoM** as the proximity of the *ortho*-CH_3 moiety clearly changes the frequency of the N–H stretching vibration). The third group consisting of **NoxM** and 5-Cl-**NoxM** displays the intramolecular N1–H1···N22 interaction as the main hydrogen bond and exhibits a typical sharp peak at around 3335 cm^{-1} (3286 cm^{-1} for **NomM** due to the additional interaction of the amide N–H with a neighbouring carbonyl oxygen). Therefore, IR spectroscopy provides a useful indicator of the type of N–H hydrogen bonding in these and related crystal structures and has been especially useful in identifying polymorphs.

3.3.2 The NpxM isomer series. The three **NpxM** isomers aggregate *via* $_{amide}$N–H···O=C C(4) chains for both **NppM** and **NpoM** isomers and through $_{amide}$N–H···$N_{pyridine}$ C(7) chains for **NpmM**.

3.3.2.1 ***NppM.*** The **NppM** isomer crystallizes in *P*2/*c* and refines initially to an *R*-factor of 0.15. Application of the twin law [100, 0$\bar{1}$0, 00$\bar{1}$] results in an *R*-factor of 5% without any non-hydrogen atom disorder apart from the CH_3 group disordered equally over two orientations. The hydrogen bonding as $_{amide}$N–H···O=C_{amide} 1D C(4) chains forms along the *b*-axis [010] direction (Fig. 1) (Table 2). There are no other strong interactions of note in an otherwise regular structure (with similarities to **NppF**).[11] The pyridine N24 atom does not participate in hydrogen bonding, with the closest intermolecular H···N24 contact distance >2.90 Å (similar to the lack of interactions for the pyridinyl N24 in **NppF**).[11]

3.3.2.2 ***NpmM.*** **NpmM** (with a **M-*anti*** tolyl ring conformation) aggregates *via* intermolecular N1–H1···N24 hydrogen bonds and assisted by a flanking C22–H22···N24 interaction forming a ring with graph set $R_2^1(7)$ (Fig. 2). This tandem effect links as a 1D column in the [010] direction; columns are linked reciprocally by longer C23–H23···O1 interactions parallel to the ($\bar{1}$01) plane into 2D rumpled sheets. All interplanar angles are <20° highlighting the near co-planarity of all atoms in **NpmM** in contrast to both of the **NppM** and **NpoM** crystal structures (Table 2).

3.3.2.3 ***NpoM.*** **NpoM** with the tolyl ring in the **M-*syn*** conformation although almost orthogonal to the amide linker (Table 2) crystallizes in space group *Cc* with N–H···O=C as the primary hydrogen bond linking along the *c*-axis or [001] direction (Fig. 3). The short N1···$O1^i$ = 2.825(2) Å is augmented by an *ortho*-CH_3···$(O=C)^i$ interaction involving the methyl group interacting with the neighbouring C=O group (symmetry code $i = x, -y, z - 1/2$) (Fig. 3). The closest intermolecular contact involving pyridyl N24 is with the aromatic H22 atom [H22···N24 = 2.72 Å]. The isomorphous **NpmF** and **NpoF** systems also crystallise in space group *Cc* but differ from **NpoM** by having N–H···$N_{pyridine}$ as the primary interaction.[11]

3.3.3 The NmxM isomer series. The three **NmxM** isomers aggregate by $_{amide}$N–H···$N_{pyridine}$ interactions for **NmpM** (**NmpFM**), **NmmM** and through $_{amide}$N–H···O=C interactions in **NmoM**.

3.3.3.1 ***NmpM*** *and the* ***NmpFM*** *mixed structure.* **NmpM** crystallises as fine needles that splinter easily. The **NmpM** crystal structure (Fig. 4a) contrasts with **NmpF** (a hydrogen bonded tetramer assembling *via* cyclical $_{amide}$N–H···$N_{pyridine}$ in space group $P\bar{1}$).[11] In **NmpM** the primary interaction that drives aggregation is also $_{amide}$N–H···$N_{pyridine}$ but is catemeric (Fig. 4b) and in the form of a stepped column with an intermolecular

View Article Online

Published on 28 April 2011. Downloaded by University of Birmingham on 30/10/2014 11:07:57.

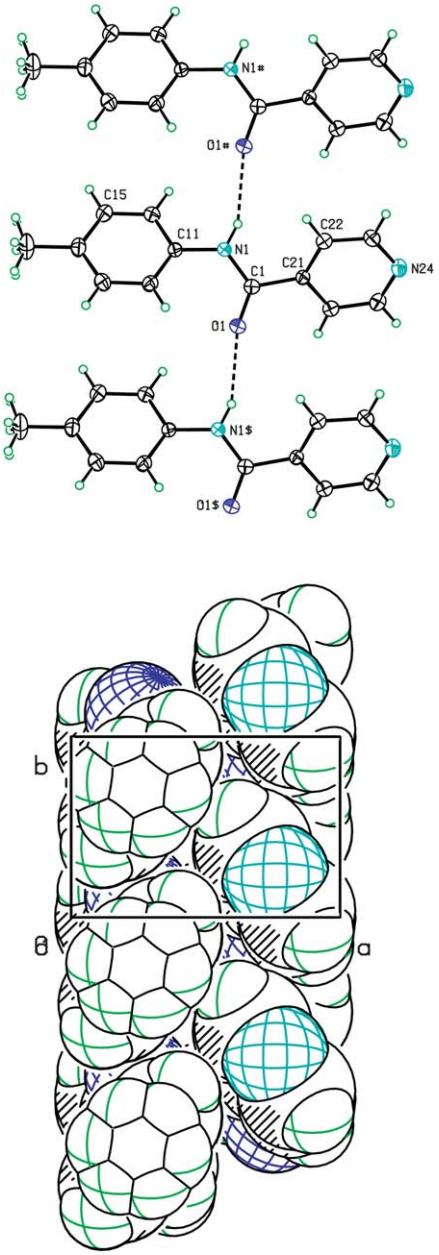

Fig. 1 (a) An ORTEP diagram of **NppM** (with displacement ellipsoids drawn at the 30% probability level) as a chain of three molecules with the primary N–H···O=C interaction aggregating along the *b*-axis direction and (b) two chains with atoms as van der Waals spheres and parallel to the (001) plane.

N···N distance of 3.223(2) Å and N–H···N angle of 164.7(12)°; the pyridinyl (**Nm**) ring has the **N-*syn*** conformation. In **NmpM** the assembly process as an N–H···N relay generates an alternating two-molecule column along the *b*-axis [010] direction, linked by weaker C–H···O=C interactions along the [001] direction (2D) and C–H···C/π(arene) contacts along the [100] direction forming a 3D structure. The key difference is that the CH_3 groups in **NmpM** form C–H···π(arene) interactions and link the stacked columns [with six C···C(arene) distances from 3.68 to 4.03 Å], whereas this does not arise as donor C–F··· (arene) interactions in **NmpF**.[11] The intermolecular data indicate

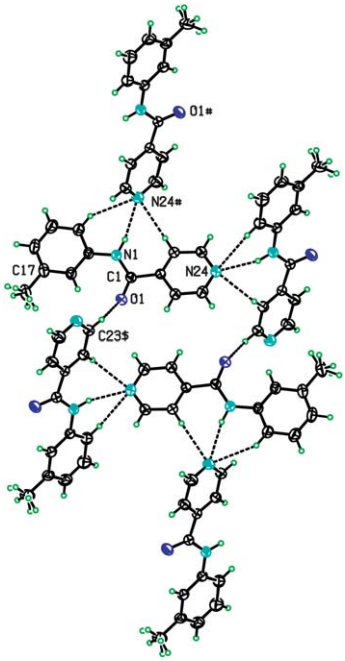

Fig. 2 An ORTEP diagram of **NpmM** as two chains with *zig-zag* primary N–H···N hydrogen bonds, C–H···N interaction/contacts and linked by C–H···O=C (displacement ellipsoids as in Fig. 1a). The suffix labels # and $ are for symmetry related sites 1/2 − *x*, 1/2 + *y*, 3/2 − *z* and −1/2 + *x*, 1/2− *y*, −1/2 + *z*.

that (at the primary interaction level) the **NmpM** and **NmpF** molecules are similar and differences between the remotely positioned CH_3/F groups influence the overall aggregation and packing. Catemeric/tetrameric aggregation interchange is known in pyrazole chemistry.[36] As both **NmpM** and **NmpF**[11] contrast in

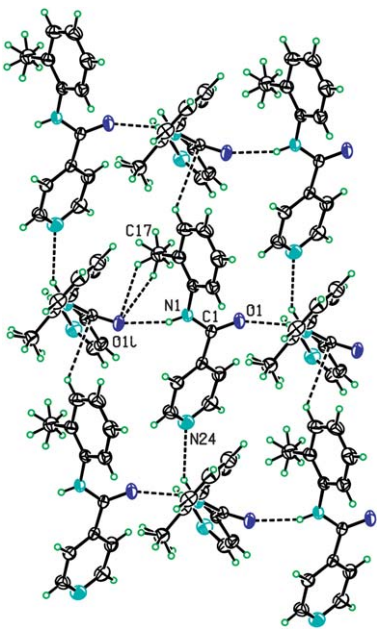

Fig. 3 An ORTEP diagram of **NpoM** with three molecules in three chains showing the primary N–H···O=C interaction propagated along the *c*-axis with weaker contacts at O1^{i} (displacement ellipsoids as in Fig. 1a).

 This journal is © The Royal Society of Chemistry 2011

View Article Online

Published on 28 April 2011. Downloaded by University of Birmingham on 30/10/2014 11:07:57.

their aggregation modes, their solution mixtures and resulting solid-state structure **NmpFM** were analysed.

A 50 : 50 solution of **NmpF** and **NmpM** (recrystallized from ethyl acetate) yields the crystal structure of **NmpFM** which differs from both **NmpF** and **NmpM**. The molecules occupy the same site in the asymmetric unit of space group $Pna2_1$ differing only by the 50 : 50% occupancy of the F14 atom and CH_3 group (Fig. 4c). **NmpFM** is comparable to both **NmpF** and **NmpM** structures in basic geometry. However, **NmpFM** is similar to **NmpM** in the primary intermolecular N–H···N/C–H···N hydrogen bonding mode but aggregation differs *via* weaker C–H···O═C by linking the columns into 2D sheets which interlock *via* weaker C–H/F···C contacts (Fig. 4d). For comparison, the N···N intermolecular distances change from 3.2205(19) to 3.285(2) Å in **NmpF**,[11] 3.223 (3) Å in **NmpM** and 3.207(3) Å in **NmpFM**.

The interchangeability of F/CH_3 moieties in crystal structures has been reported in the 5-fluorouracil : thymine crystalline solid solution.[37,38]

3.3.3.2 ***NmmM***. The **NmmM** structure ($Z' = 2$) is *essentially* isomorphous and isostructural with **Mmm**,[10] the *amide reversed* or '*bridge-flipped*' related isomer (Fig. 5a and b). The **NmmM** unit cell parameters of 9.38, 9.92, 12.34 Å, 86.96°, 86.98°, 71.41° [RT] are similar to the unit cell data of **Mmm** (a *non-merohedral* twin) of 9.59, 9.99, 12.51 Å, 85.83°, 85.77°, 68.56° [at 294(1) K]. The ring conformations in **NmmM** are **N-*anti*/M-*anti*** (Fig. 5a and b) and for **Mmm**[10] are **M-*anti*/P-*anti***. Comparisons between molecules A and B reveal C_6/C_5N interplanar angles of 57.23(6)°, 54.76(6)° in **NmmM**, and 55.57(10)°, 65.70(10)° in **Mmm**.[10] For **NmmM** the primary N–H···N hydrogen bonding distances are 3.090(2), 3.078(2) Å and longer than 2.998(4) Å, 3.006(4) Å in **Mmm**.[10] In **NmmM**, 1D chains are linked by C–H···O interactions into 2D sheets parallel to (110). Analysis of structural isomers differing by a '*bridge flip*' (with **NmmM** and **Mmm**[10] as reversed amides) provides a perspective beyond analysis of the individual molecules. Comparisons of two $n \times m$ isomer grids can *potentially* yield invaluable structural information especially

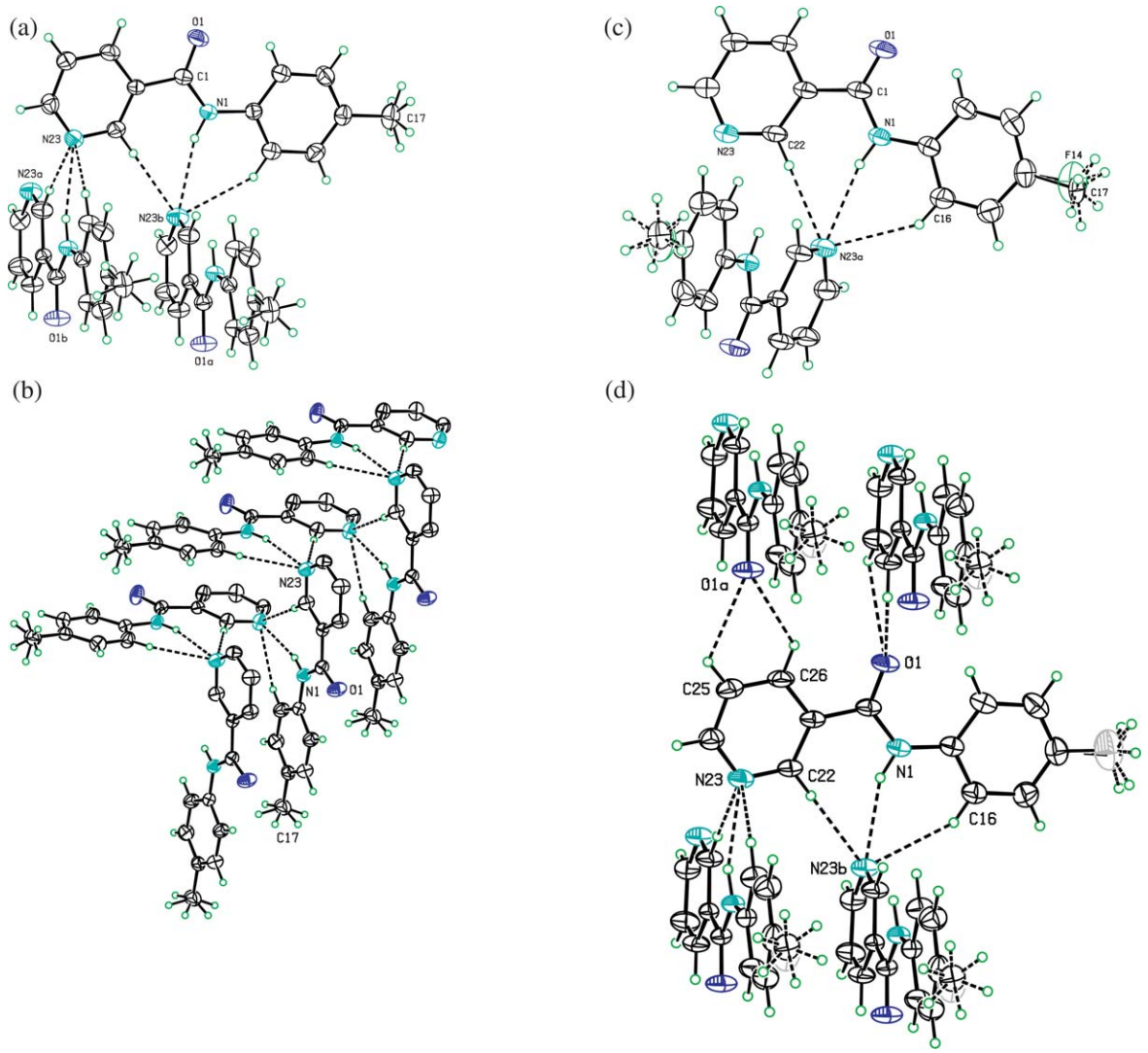

Fig. 4 An ORTEP diagram of **NmpM** as (a) three molecules with N/C–H···$N_{pyridine}$ interactions (at sites $a = -x, 1/2 + y, 1/2 - z$; $b = -x, -1/2 + y, 1/2 - z$), (b) a catemeric linked column (displacement ellipsoids as in Fig. 1a) and with pyridyl H atoms omitted for clarity. (c and d) An ORTEP view of two **NmpFM** molecules and the primary C/N–H···$N_{pyridine}$ [$R_2^1(6)$, $R_2^1(7)$ rings] and C–H···O═C interactions [$R_2^1(5)$ rings] in **NmpFM**.

View Article Online

Published on 28 April 2011. Downloaded by University of Birmingham on 30/10/2014 11:07:57.

when *isomorphous* pairs are found. Ojala and co-workers[14] have reported that isostructural relationships exist with halogen replacement (X = F, Cl, Br, I) in a benzylideneaniline series, but *not* with the *bridge-flipped* isomers (as –CH=N– *vs.* –N=CH–). They stated that '*in general isostructuralism between bridge flipped isomers is rare. Differences between the isomers with respect to their molecular conformations and solid-state intermolecular interactions tend to differentiate their solid-state molecular packing arrangements*'. Herein, **NmmM** and **Mmm**[10] provide a rare example of *isostructuralism* in *bridge-flipped* isomers (Fig. 5a and b).[10]

The melting point range is 113.0–114.7 °C in **NmmM** and 90.0–91.0 °C in **Mmm**, a difference of *ca.* 23 °C. However, **Mmm** is twinned (0.844 : 0.156) and despite the isostructural nature of these isomers, **Mmm** has fewer interactions and contacts due to the absolute and specific nature of the packing. This may account for the disparity in mp ranges. Comparisons of *bridge-flipped* isomers can provide information that polymorphs often cannot, as polymorphic forms *usually* differ substantially in packing and *often* with different Z'.[5]

We reported the **3,4-F$_2$** and **3,5-F$_2$** difluorobenzamide isomers[39] are *essentially* isomorphous structures (similar unit cells and gross packing) but with distinctly different primary hydrogen bonding distances due to the packing at the atom/group/ring level arising from differences in the peripheral ring substitution patterns of the **3,4-F$_2$** and **3,5-F$_2$** systems. Increasing numbers of related structures will provide more examples for future analysis and correlation.

3.3.3.3 ***NmoM.*** **NmoM** forms $_{amide}$N–H···O=C$_{amide}$ interactions along [010] as the primary hydrogen bond augmented by weaker C–H···π(arene) interactions from C24 and C26. The ring conformations in the crystal structure are **N-*anti*/M-*anti***.

In **NmoM** the *meta*-pyridinyl N23 atom does not form hydrogen bonds (positioned where no donor atom can interact) with closest contact from N23···H25 = 2.95 Å [H25 at symmetry position $-1/2 - x$, $1/2 + y$, z].[31] **NmoM** is isostructural with related benzamides[41] [defined as C$_6$CONHC$_6$] that do not possess a pyridine acceptor group. This may explain the isostructurality of **NmoM** with benzamides [such as PIFLAS, QOVDOV, POPWUN][5] that all crystallise in space group *Pbca* (No. 61) with similar unit cell parameters. Analysis of isomeric series of mono- and dichloro-/methyl benzamides[5,41] reveals a preponderence of C$_6$CONHC$_6$ structures in *Pbca* with similar unit cell parameters *i.e.* $a, b = 6 \rightarrow 10$ Å, $c = 20 \rightarrow 30$ Å. The **NmoM** structure (with pyridyl N23 atom) is expected to form intermolecular N–H···N/C–H···N interactions on crystallisation. The lack of N···N hydrogen bonding means that **NmoM** mimics the more common N–H···O=C hydrogen bonding motif in benzamides. Of further note is that **NmoM** with unit cell data of 8.07, 9.40, 29.53 Å and mp range of 106.1–107.0 °C is *isomorphous* with the bromo derivative **TICDOZ**[40] [unit cell parameters of 8.15, 9.35, 29.59 Å; mp = 92 °C]. Overlap of **NmoM** and **TICDOZ**[40] shows the main differences are due to the C–Me and C–Br moieties (Fig. 6). Both structures have almost orthogonal C$_6$/C$_5$N rings and the **TICDOZ** torsion angles are all within 3° of the related angles in **NmoM**.

3.3.4 The NoxM isomer series. A variation of 0.08 Å is noted in the intramolecular N1···N22 interaction distance from 2.6548 (18) Å [torsion angle N1–C1–C21–N22 = 3.87(18)°, **NopM**],

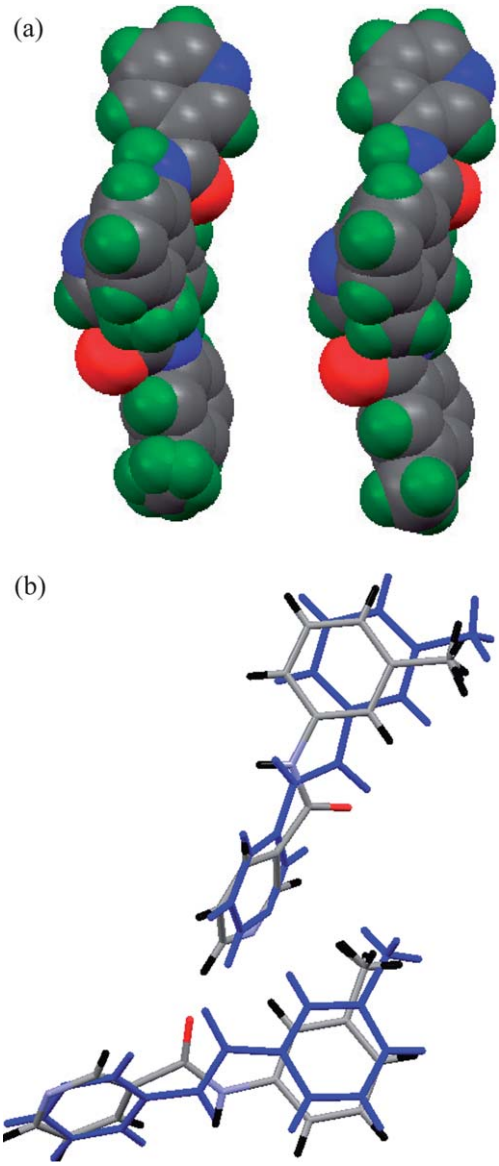

Fig. 5 (a) **NmmM** and **Mmm** molecules depicted as their van der Waals spheres and highlighting the similarity of the asymmetric unit. (b) **NmmM** overlaid with (**Mmm**[10] in blue).

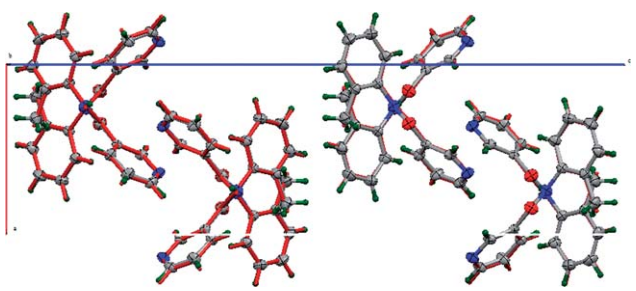

Fig. 6 A unit cell packing view along the *b*-axis direction of **NmoM** (ellipsoids) with **TICDOZ**[40] (related bromo derivative in red) as a ball and stick model (displacement ellipsoids for **NmoM** as in Fig. 1a).

 This journal is © The Royal Society of Chemistry 2011

View Article Online

Published on 28 April 2011. Downloaded by University of Birmingham on 30/10/2014 11:07:57.

2.683(4), 2.704(4) Å [angles (A) = 2.2(3)°, (B) = 17.5(4)°] in **NomM** and 2.6209(15) Å [0.45(14)°] in **NooM**. Aggregation typically occurs *via* C–H···O=C intermolecular interactions; however, the interaction mode in **NomM** is *rather* unexpected.

3.3.4.1 ***NopM***. **NopM** is a regular structure (having the **No** ring conformation as **N-*syn***) with N1–H1···N22 and a C–H···O=C intermolecular interaction (from C16) linking molecules into alternating 1D columns along the *a*-axis parallel to the (001) plane (Fig. 7), but stacked (in an alternating fashion) along [001]. Weaker C–H···O=C (from C23) links columns into 2D sheets with *para*-substituted methyl groups interlocking with neighbouring sheets by van der Waals and π···π stacking contacts.

3.3.4.2 ***NomM***. Two molecules in the asymmetric unit (Z' = 2) differ in **NomM** (Fig. 8a and b) (Table 2). The unexpected N–H···O=C intermolecular interactions with $N1_{A/B}\cdots O1_{B/A}$ = 3.241(3), 3.132(3) Å are longer than the N···O distances in **NppM**, **NpoM** and **NmoM**. In **NomM** the amide···amide interaction (H···O = 2.32, 2.42 Å) in tandem with a C–H···O=C contact forms a hydrogen bonded $R_2^1(6)$ ring per molecule and overall as 2D sheets. Molecules A and B differ significantly with torsion angles for O1–C1–C21–N22 = −176.0(3)°, −162.6(3)° (Table 2); however, both molecules exhibit the **N-*syn*/M-*anti*** conformation. The aggregation in **NomM** is unusual compared to the other eight **NxxM** isomers and this is evident with **NomM** forming the poorest quality crystals of an isomer that proved reluctant to crystallise; the interactions are weak and often repulsive. Of the **NxxM** isomers it has the lowest mp range of 49–50 °C and an explanation for the low mp is that molecules are positioned with only a modest amount of energy needed to force the molecules to 'slip' or break up the intermolecular N–H···O=C interactions near/at the melt event.

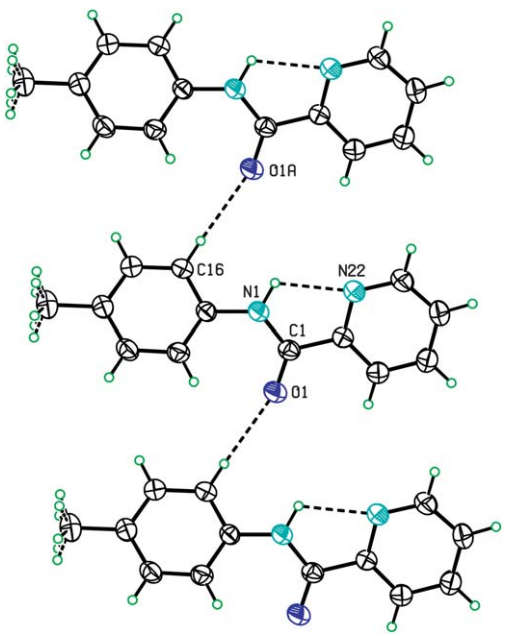

Fig. 7 Three molecules of **NopM** showing the N–H···N intramolecular and primary C–H···O=C interactions along the *a*-axis direction involving C16 (displacement ellipsoids as in Fig. 1a).

3.3.4.3 *The elusive* ***NooM***. **NooM** crystals proved to be the most elusive of the nine **NxxM** isomers and were subject to many crystallisation attempts yielding gel-like, plastic spirals. Suitable crystals were eventually grown after several trials using methanol. **NooM** with the intramolecular N1–H1···N22 interaction forms a hydrogen bonded dimer *via* the C15–H15···O1a interaction about inversion centres [C15···O1a = 3.4720(16) Å] (Fig. 9). Dimers do not pack efficiently and the effective *dimer* is only slightly *stepped* in appearance and there are no other interactions of note (the molecular volume is average for **NxxM**). The lack of interactions directly impacts on packing and obviously leads to the lack of initial success with obtaining quality crystals of **NooM**. The structure of **NooM** is planar with conformation **N-*syn*/M-*syn*** and C_6/C_5N interplanar angles of 1.91(5)° and all interplanar angles involving the aromatic rings and the amide linkage are <2°. The amide C1–N1–C11 angle of 131.02(11)° is larger than the equivalent C1–N1–C11 angles in the **NxxF** and **NxxM** isomers with C–N–C angles from 123° to 129° noted. The N1–C1–C21 angle in **NooM** is 112.71(11)° and

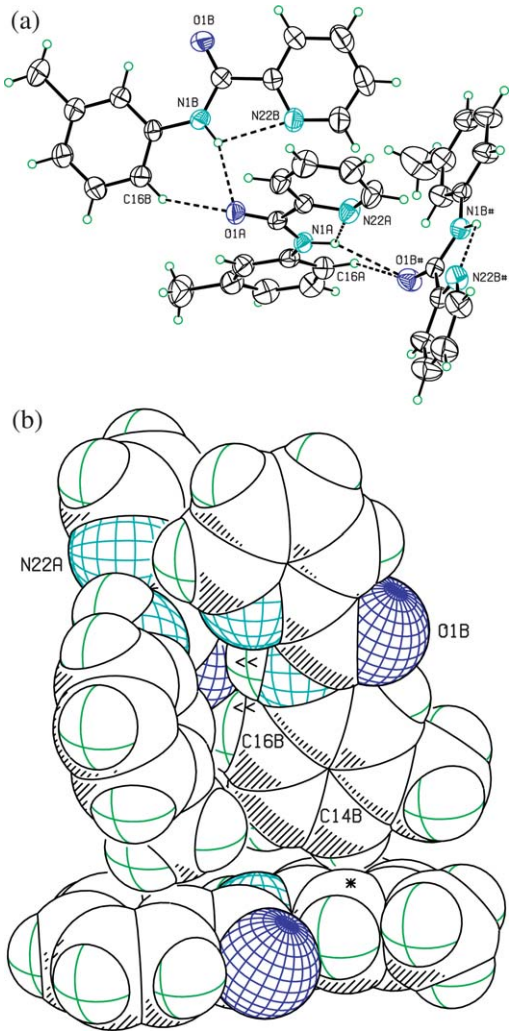

Fig. 8 (a) An ORTEP view of three **NomM** molecules highlighting the unusual packing and contacts (displacement ellipsoids as in Fig. 1a) with symmetry code # = −*x*, 1/2 + *y*, −*z* and (b) the intimate packing with ≪ showing the orthogonal nature of the C16B–H16B/N1B–H1B···O1A=C1A interactions and with * for the C14B–H14B···π(arene) interaction.

View Article Online

Published on 28 April 2011. Downloaded by University of Birmingham on 30/10/2014 11:07:57.

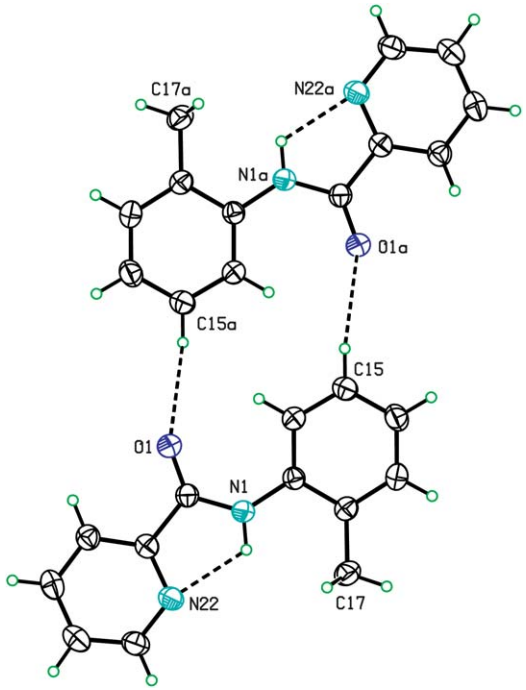

Fig. 9 An ORTEP view of the dimeric unit in **NooM** along the *a*-axis direction with centrosymmetric C–H···O=C interactions as dashed lines and suffix $a = 1 - x, 1 - y, 1 - z$ (displacement ellipsoids as in Fig. 1a).

acute compared with the 113 to 119° range in related **NxxM** isomers. These two angles are similar to the 5-Cl-**NopM** and 5-Cl-**NooM** molecules and primarily due to steric effects on adopting planarity.

3.3.5 Three 5-Cl-NoxM isomers. The 5-Cl-**NoxM** compounds were isolated as minor components from their respective **NoxM** reactions and yielded crystalline solids. 5-Cl-**NopM** crystallises as an inverted twin in space group $Pca2_1$ with twin component ratios of 0.87 : 0.13. The 5-Cl-**NopM** molecule is not planar (Table 2) and participates in weak interactions with the intramolecular N1···N22 = 2.6514(9) Å. Two additional weak C–H···O1=C1 interactions are present with C12···O1 = 2.9543(11) Å (intramolecular) and 3.4223(11) Å (C23, intermolecular and C16). A π···π stacking interaction is observed with C1···C24a = 3.3312(13) Å, and C17 forms a weak C–H···π (arene) interaction with the [C11, …, C16] aromatic group (Fig. 10). The 5-Cl-**NomM** crystal is also twinned with twin components of 0.972 : 0.028 and refinement drops the *R*-factor from 7.5% to 6.6%. The principal interaction is N–H···O=C at 3.035(4) Å and shortest stacking interaction is C21···C12a at 3.338(4) Å [$a = x, 3/2 - y, 1/2 + z$].[31] The N–H···O=C hydrogen bond is unorthodox and the effect of the combination of N–H···O=C/π···π stacking interactions is to generate a stacked complex as a 1D column propagating along the *c*-glide plane (Fig. 11). Finally, the 5-Cl-**NooM** structure contains the intramolecular N1···N22 = 2.6690(15) Å interaction with an intramolecular contact C16···O1 = 2.9128(19) Å. The other relevant interaction is C26–H26···Cl1^{i} where C26···Cl1^{i} = 3.7371(14) Å ($i = 1/2 - x, 1/2 + y, 1/2 - z$). Molecules are linked along [100] as a 1D molecular tape (Fig. 12).

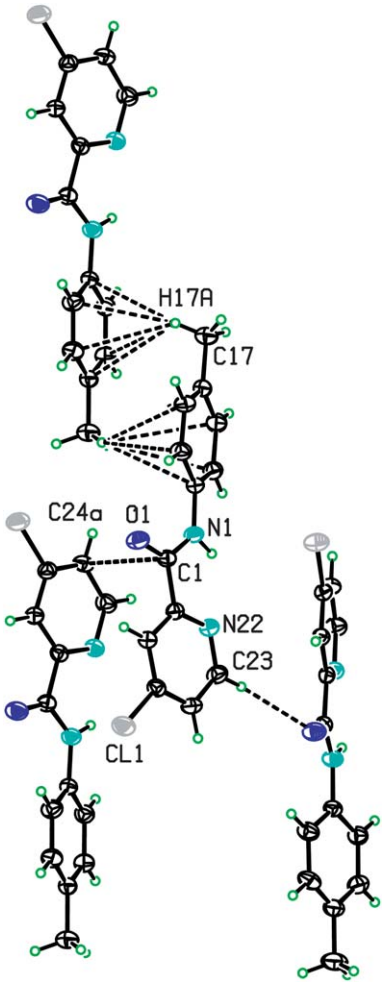

Fig. 10 A view of the intermolecular interactions in 5-Cl-**NopM** with label suffix $a = 1/2 + x, -y, z$ (displacement ellipsoids as in Fig. 1a).

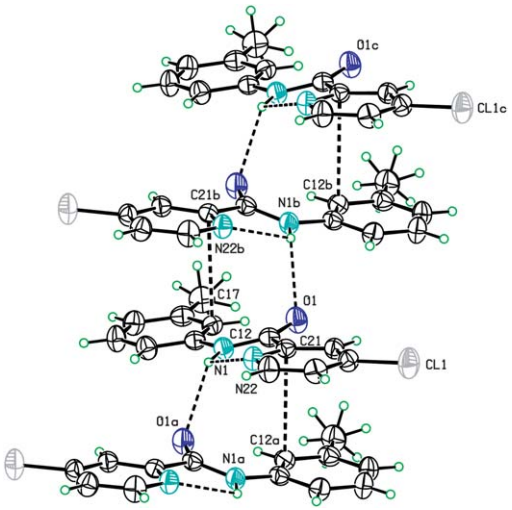

Fig. 11 A view of the primary N–H···O=C intermolecular interactions in 5-Cl-**NomM** with π···π stacking depicted for C21···C12a; suffixes *a*, *b*, *c* refer to the symmetry related sites: $x, 3/2 - y, -1/2 + z$; $x, 3/2 - y, 1/2 + z$ and $x, y, 1 + z$ (displacement ellipsoids as in Fig. 1a).

 This journal is © The Royal Society of Chemistry 2011

View Article Online

Published on 28 April 2011. Downloaded by University of Birmingham on 30/10/2014 11:07:57.

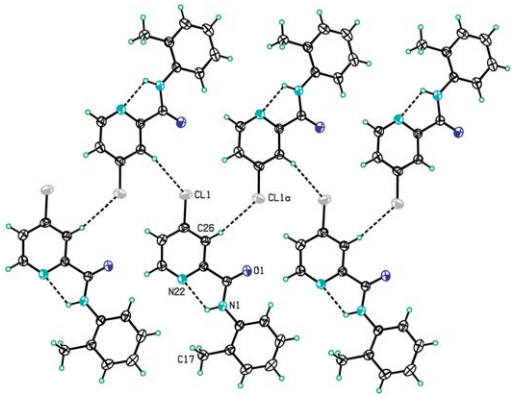

Fig. 12 A view of the C–H···Cl interactions along the *b*-axis in the 1D molecular tape of 5-Cl-**NooM** (displacement ellipsoids as in Fig. 1a).

3.4 Melting point analysis and structural results summary

The melting point data in Table 3 show the general trends in three isomeric series that differ by a *reverse amide* bridge and replacement of CH_3 group by a F atom along the series **Mxx** ↔ **NxxM** ↔ **NxxF**. The comparisons are detailed as:

(a) The overall trend is from the symmetrical *para*/*para* substituted (**pp**) isomers with typically the highest melting points to those with the lowest melting points which are usually a combination of *ortho*/*meta* (**o/m**).[9–11] In each triad the mp range decreases from $p \rightarrow o$ but for **NoxM** and 5-Cl-**NoxM** this trend is not adhered to with the **mM** substituent having the lowest melting point. The **Mmo**, **NomM** and **NomF** compounds have the lowest mp ranges in each of the three series.[10,11] They possess an *ortho*-N_{pyr} in combination with a *meta*-**Me/F** substituent and this combination is a good predictor of a lower than average mp in each of the three series.[10,11] For **NomM** the lowest melting point also coincides with the largest molecular volume at 295 Å^3 (and lowest density) as well as unusual aggregation (Tables 1 and 2).

(b) The vast majority (80%) of the isomers have the $_{amide}$N–H···$N_{pyridine}$ rather than N–H···O=C as the primary interaction though not in any way that can be easily predicted, nor is there any general correlation between either type of interaction and the melting point. However, the mp trends show **NxxM** to be similar to **NxxF**, but the hydrogen bonding type in **NxxF** more closely resembles **Mxx** with 8 of 9 isomers having $_{amide}$N–H···$N_{pyridine}$ as the primary interaction.

(c) For **NmpF**, **NmpM** and **NmpFM** the volumes are 253 Å^3, 269 Å^3 and 266 Å^3 with the latter two aggregating *via* catemeric assembly as distinct from the tetramers in **NmpF**.[11] The **NmpF** and **NmpFM** (132–134 °C) mp data are similar.

(d) The 5-Cl-**NoxM** derivatives have higher melting points as compared to their **NoxM** relatives and by >20 °C; this effect is due to replacement of H by Cl.

3.5 *Ab initio* calculations

3.5.1 Structure optimisations. The key structural features of the **NxxM** isomers optimised in the *gas phase* and solvents are presented in Table 4, including the α, β and amide linkage dihedral angles δ [O1=C1–N1–C11]. The most salient feature of the geometry analysis is the planarity of the **NoxM** triad in contrast to the **NpxM**, **NmxM** isomers, For **NoxM**, all dihedral angles are equal to or close to 0°, with or without the solvation model and therefore only the **NpxM** and **NmxM** triads are discussed.

Table 3 Mp data for **Mxx**, **NxxF** and **NxxM** series[ab]

	Mxx			**NxxM**			**NxxF**			
	p	m	o	Np	Nm	No	Np	Nm	No	
Mp	*181*	**128**	*105*	**162**	*148*	*105*, ***128***	**135**	*132*	*94*	pF/M
Mm	*106*	*91*	*79*	*142*	*114*	**50**, ***72***	*132*	*122*	*78*	mF/M
Mo	*129*	*108*	*116*	**125**	**107**	*65*, ***128***	*140*	*117*	*107*	oF/M

[a] The mid-point of the melt (°C) is quoted. [b] Italic values refer to the N–H···N_{pyr} and bold values refer to the amide···amide interactions; the 5-Cl-**NoxM** mp data are represented as bold italics (mid-table).

For the **NpxM**, **NmxM** isomers (*gas phase*) the dihedral angles exhibit a regular pattern. The α angle is 26.76 ± 0.09° in **NpxM** and 24.56 ± 0.09° in **NmxM**. The β angle is 5.69 ± 0.07° in **NpoM** and **NmoM** while the remaining four structures have β = 3.65 ± 0.43°. However, the δ dihedral angle increases slightly from 3.17° (**NppM**) to 3.77° (**NmoM**).

The dihedral angles optimised in CH_2Cl_2 display a different though somewhat less regular pattern. The α angle in **NpoM**, **NmoM** is 31.66 ± 0.41° while the remaining four are 27.78 ± 1.3°. The β angle in **NppM**, **NmpM** is 5.52 ± 0.52°, for **NpmM**, **NmmM** = 2.91 ± 0.33°, whereas in **NpoM**, **NmoM** β = 10.01 ± 0.13°. The δ angle shows a small regular increase from 2.13° (**NppM**) to 5.24° (**NmoM**).

The α dihedral angle optimised in H_2O for all **NpxM**/**NmxM** isomers is 29.66 ± 0.85°, while δ increases from 2.15° to 3.44°. For β, both **NpoM** and **NmoM** exhibit a deviation of 40.41 ± 0.01° compared to the remaining four at 11.23 ± 2.08°. For the **NxxM** isomers optimised in the *gas phase* this deviation is small, while slight deviations exist for the optimised structures in CH_2Cl_2. In general, the **NoxM** triad is planar (due to the intramolecular N–H···N) and the molecular distortion of the remaining **NxxM** structures occurs through rotation of the pyridine ring (*gas phase*) and both pyridine (**N**) and tolyl (**M**) rings (in solvents). Crystallographic and spectroscopic results support this interaction.

Table 4 Torsion angles (°) of the optimised **NxxM** isomers[a]

	Optimised in *gas phase*			Optimised in CH_2Cl_2			Optimised in H_2O		
	α	β	δ	α	β	δ	α	β	δ
NppM	26.65	3.70	3.17	26.62	5.89	2.13	28.81	11.07	2.15
NpmM	26.80	3.58	3.18	27.57	3.14	2.06	28.39	8.34	2.32
NpoM	26.83	5.64	3.32	31.95	9.91	4.54	30.40	40.40	2.67
NmpM	24.60	4.19	3.39	29.63	5.15	3.54	29.90	12.59	3.11
NmmM	24.45	3.14	3.67	27.29	2.67	2.77	30.09	12.91	3.28
NmoM	24.62	5.75	3.77	31.37	10.10	5.24	30.38	40.42	3.44
NopM	0.00	0.00	0.00	0.00	0.00	0.00	0.00	0.00	0.00
NomM	0.00	0.00	0.00	0.00	0.00	0.00	0.00	0.00	0.00
NooM	−0.01	0.00	0.00	0.00	0.00	0.00	−0.01	0.00	−0.02

[a] The angle C26–C21–C1=O1 (**N**-ring) is designated as α; the C1–N1–C11–C12 angle (**M**-ring) as β and the O1=C1–N1–C11 angle (amide linkage) as δ. All geometries are based on B3LYP/6-311++G optimisation with PCM-SMD solvation model.

View Article Online

Published on 28 April 2011. Downloaded by University of Birmingham on 30/10/2014 11:07:57.

3.5.2. Conformational analysis. Fig. 13 depicts the nine PES conformational analysis diagrams of the **NxxM** modelled structures in the *gas phase*. The **N**-ring (pyridinoyl ring, α dihedral angle) is drawn as a full red line, with the **M**-ring (tolyl ring, β dihedral angle) as a blue dashed line. At $\theta = 0$ and $\pm 180°$, the conformation of the asymmetric **N**- or **M**-ring is noted as ***syn*** or ***anti***. Higher resolution PES diagrams are provided in the ESI† with a detailed description (Section 5.2). The modularity of the **NxxM** isomer series is highly expressed, with each **N** or **M** ring (*p*-, *m*- or *o*-) having a distinctive PES curve.[10,11]

The *para*-pyridine (**Np**) ring is symmetrical, with all stable conformations energetically equal. For the *meta*-pyridine ring (**Nm**) the preferred conformation is **N-*syn***. The difference on changing to **N-*anti*** is 4.70 ± 0.17 kJ mol^{-1}; Boltzmann distribution of the different conformers indicates that ~86% of all molecules at 294 K have the **Nm** ring in the **N-*syn*** conformation with the remainder in the **N-*anti*** conformation. The *ortho*-pyridine (**No**) ring exhibits a symmetrical PES curve and strongly favours the **N-*syn*** conformation where the intramolecular N–H···N hydrogen bond forms.

Both the *para*-tolyl (**pM**) and the *meta*-tolyl (**mM**) provide symmetric PES curves. Although the **M-*anti*** conformation in the **mM** ring is the slightly preferred conformation, the 0.37–0.46 kJ mol^{-1} energy difference when compared to the **M-*syn*** conformation ensures both conformations are plausible. The *ortho*-tolyl (**oM**) shows a strong preference for the **M-*syn*** conformation. However, both **NpoM** and **NmoM** have asymmetric PES curves, whereas the planar **NooM** has a symmetrical curve. Although the **M-*syn*** conformation is preferred, deep potential wells at the local minima (LM_{oM}, 5–7.5 kJ mol^{-1}) can cause another conformation closer to **M-*anti*** to occur to a minor extent.

Overall, the *gas phase* conformational analysis shows that the favoured **NxxM** conformation is **N-*syn*/M-*syn*** for the majority of asymmetric rings (structures), but excluding the **NxmM** triad, where the preferred conformation is **N-*syn*/M-*anti***, albeit the difference with **N-*syn*/M-*syn*** is small with both conformations possible.

The conformational analysis results using the PCM-SMD solvation model (CH_2Cl_2 and H_2O as solvents) are given in the ESI† along with detailed descriptions and explanations (Section 5.3). Introduction of the solvent model does not cause a major conformational change in the modelled **NxxM** structures (***syn*–*anti*** model) in the *gas phase*; asymmetric **NxxM** isomers have the **N-*syn*/M-*syn*** conformation with the **NxmM** triad being **N-*syn*/M-*anti***. As reported by us previously,[10,11] the general feature of the solvated conformational analysis is a decrease in rotational barriers. However, when specific rings are coplanar with the amide linker an increase is noticed. The reason for the increase is an increase in repulsion factors due to the higher dielectric field.

It is important to note that deviations of the *ortho*-tolyl rings (β dihedral angle) in **NpoM** and **NmoM** (as discussed in Section 3.5.1) are the major cause of shifts in the corresponding PES

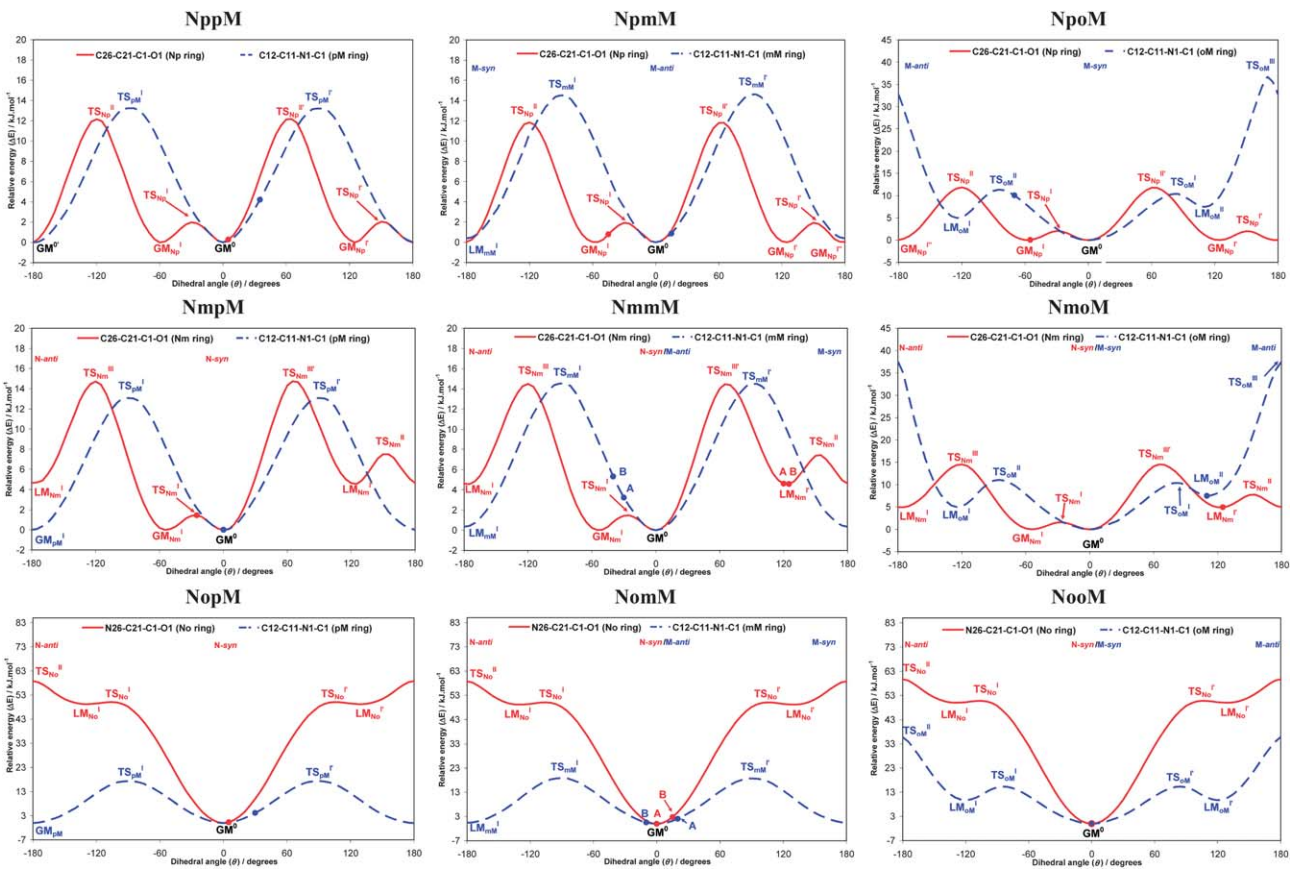

Fig. 13 The PES conformational analysis for the nine **NxxM** isomers optimised in the gas phase: the equivalent solid state angle is depicted by (●) with, if applicable, an assigned identification letter. High resolution figures and descriptions are provided in the ESI†.

 This journal is © The Royal Society of Chemistry 2011

View Article Online

Published on 28 April 2011. Downloaded by University of Birmingham on 30/10/2014 11:07:57.

curves. This effect is more pronounced in the more polar solvent (H_2O) allowing unexpected conformations to be isolated.

Another notable effect is the significant decrease in energy (both local minima and transition states) when the *meta*-pyridine (**Nm**) ring is in the **N-*anti*** conformation and by a linear decrease of ~3.35 kJ mol^{-1} in CH_2Cl_2 (~3.87 kJ mol^{-1} in H_2O). This results in a small energy gap between the **N-*syn*** and **N-*anti*** conformations of the **Nm** ring, 1.45 kJ mol^{-1} in CH_2Cl_2 (0.38 kJ mol^{-1} in H_2O). From the Boltzmann distribution, at 294 K approximately 35% of the molecules in CH_2Cl_2 and approximately 47% of the molecules in H_2O have the **Nm** ring in the **N-*anti*** conformation. Therefore, conformational analysis with the PCM-SMD solvation model predicts the plausibility of the **N-*anti*** conformation of the **Nm** ring. A similar effect in the **mM** ring arises, but the energy difference between **M-*anti*** and **M-*syn*** in CH_2Cl_2 is *just* 0.21 kJ mol^{-1}, while in H_2O the difference is negligible (0.03 kJ mol^{-1}), making both conformations energetically equal. This implies that the **mM** ring in polar solvents can potentially adopt both **M-*anti*** and **M-*syn*** conformations equivalently.

Although the **NxxM** isomers are insoluble in H_2O, it was used as an example of a strong polar solvent ($\varepsilon_r = 80$) to illustrate and amplify solvation effects with implicit polar solvent in the PCM-SMD model; extrapolations can be made for polar solvents in which the **NxxM** isomers are soluble. Spectroscopic data demonstrate that solvents such as DMSO can disrupt intramolecular hydrogen bonding in the **NoxM** series.

4. Comparison of calculated and experimental NxxM isomer structures

Comparison of the **NxxM** isomer structures from crystal structure data and calculations is made by marking (as ●) torsion angle differences ($\Delta\theta$) between the experimental and theoretical structures on the corresponding *gas phase* PES diagrams (Fig. 13). For **NmmM** and **NomM** with $Z' > 1$ the corresponding angles are labelled as A or B. This method allows an easy visualisation and quick evaluation of structural differences between the two structure analysis approaches. Most crystallographic dihedral angles correlate with their computational counterparts by having similar conformations with an average offset of torsion angles of ±20° to 40°. This holds for the **NoxM** triad with **NooM** having both a planar crystal and calculated molecular structure. Generally, no significant differences ($\Delta\theta$) are seen in the **NoxM** isomers.

The 5-Cl-**NoxM** side products were not subjected to conformational analysis; their crystal structure conformations generally correspond with the optimised models of the related **NoxM** isomers.

In the **NpxM** crystal structures, the **Np**-ring conformation corresponds with its optimised *gas phase* model; however, it can found in either the GM^0 or GM_{Np} equivalent positions. In the case of the **NmxM** isomers the **Nm**-ring adopts the unstable $TS_{Nm}{}^{I}$ position in **NmpM** or $LM_{Nm}{}^{I'}$ in both **NmmM** and **NmoM** (Fig. 5 and 6). The unstable planar conformation of the **Nm**-ring in both **NmpM** and **NmpFM** crystal structures is due to the catemeric chain formation driven by N–H···N/C–H···N hydrogen bonding (in Section 3.3.3.1). The **No**-ring conformations in the **NoxM** crystal structures correspond with their modelled equivalents.

In almost all molecules with the exception of **NpoM** and **NmoM**, the **M**-ring conformation is the same in both the solid state and optimised *gas phase* models with a maximum deviation of ±40°. In fact all **NxmM** crystal structures have the **mM**-ring as **M-*anti*** as predicted by conformational analyses despite the small differences with the **M-*syn*** structure (0.37–0.46 kJ mol^{-1}, Section 3.5.2). This is the reverse of the **NxmF** isomers where opposite conformations and/or disorders are noted.[11]

Generally, for the **Nm**-ring the main conformational differences are seen in the **NmmM** and **NmoM** isomers. The calculated **NmmM** conformation is **N-*syn*/M-*anti***, whereas the solid state ($Z' = 2$) has a *meta*-stable **N-*anti*/M-*anti*** conformation for both molecules (Fig. 5 and 6), with A and B residing in the $LM_{Nm}{}^{I'}$ potential well (Fig. 13). There is a high probability of the **N-*anti*** conformation (Section 3.5.2) especially in polar solvents, allowing isolation of this conformation in the solid state. The reverse arrangement of the **N**-ring solid state conformation as **N-*syn*** would not facilitate the $_{amide}N–H\cdots N_{pyridine}$ hydrogen bond and would introduce short H···H sterically hindered contacts in the crystal structure (if allowed); the N–H···N interactions are crucial for the formation of the crystal structure backbone. The same phenomenon exists for the structurally similar **Mmm** and **NmmF**.[10,11]

For **NmoM** the crystallographic conformation is **N-*anti*/M-*anti*** and opposite to the **N-*syn*/M-*syn*** in the modelled structure (Fig. 13, *meta*-stable potential wells at $LM_{oM}{}^{II}$ and $LM_{Nm}{}^{I'}$). As for **NmmM**, conformational analysis shows the **N-*anti*** conformation is likely especially in polar solvents (Section 3.5.2), while the **M-*anti*** conformation can be expected as well (Section 5.3, ESI†). The primary interaction of **NmoM** is N–H···O=C which generates a 1D chain along the *b*-axis. In this arrangement the *ortho*-CH_3 group is positioned as **M-*anti*** because the alternate **M-*syn*** conformation brings the CH_3 group closer to the N–H···O=C interaction and effects a steric clash. Therefore, the $LM_{oM}{}^{II}$ potential well represents the only *niche* available for the relatively sterically bulky *ortho*-CH_3 group (compared to H). Similarly, the N_{pyr} is located as **N-*anti***, as the opposite **N-*syn*** conformation negates some weak but favourable C–H···π interactions and places it too close to the carbonyl C atom of a neighbouring molecule.

For comparison **NpoM** has N–H···O=C as the primary interaction (as in **NmoM**). In **NpoM** the *ortho*-CH_3 is positioned as **M-*syn*** but in a highly distorted and relatively *unstable* conformation, being almost orthogonal to the amide linker. However, conformational analysis with the PCM-SMD solvation model suggests that this conformation in polar solvents may be plausible (Section 5.3, ESI†). For **NpoM** the *ortho*-methyl group also participates in crystal structure formation making additional weak C–H···O=C contacts with the C=O of an adjacent **NpoM** molecule (C17 in Fig. 3).

5. Conclusions

The 3 × 3 isomer grid of the nine pyridinecarboxamides (**NxxM**) has been examined with spectroscopic methods, *ab initio* modeling and conformational analyses in *gas phase* and PCM-SMD solvent models and crystal structure analyses. In addition,

View Article Online

Published on 28 April 2011. Downloaded by University of Birmingham on 30/10/2014 11:07:57.

three 5-Cl-**NxxM** structures are reported together with **NmpFM**, a crystalline solid solution comprising a 50 : 50 mixture of **NmpM** and **NmpF**.[11]

Three **NppM**, **NpoM** and **NmoM** isomers aggregate *via* $_{amide}$N–H···O=C hydrogen bonding whereas **NpmM**, **NmpM** and **NmmM** interact *via* $_{amide}$N–H···N$_{pyridine}$ interactions. All three **NoxM** display intramolecular $_{amide}$N–H···N$_{pyridine}$ hydrogen bonds with aggregation by C–H···O=C interactions (**NomM** has intermolecular N–H···O=C interactions). For the 5-Cl-**NoxM** triad, only 5-Cl-**NomM** aggregates *via* $_{amide}$N–H···O=C (shorter N···O than **NomM**); this effect is seen with lower melting points and crystallisation difficulties.

The **NmpM** structure uses a similar primary hydrogen bonding pattern as **NmpF**[11] but *via* catemeric chains instead of tetramers.[11] A mixture of **NmpM** and **NmpF** gives **NmpFM**, a crystalline solid solution with 50 : 50% F/CH$_3$ occupancy and with N–H···N/C–H···N hydrogen bonding forming catemeric chains. Of particular note is **NmmM** which is isomorphous and isostructural with **Mmm**[10] and is a rare case of *isostructuralism* between *bridge-flipped* isomers.[13,14]

Conformational analyses on *gas phase* and solvation models have enabled comparisons of optimised geometries with solid state molecular structures, highlighting unusual solid state conformations and relations with the aggregation processes. Future research will finalise the four fluoro/methyl benzamide/pyridinecarboxamide series of 3 × 3 isomer grids, as well as explore related $n \times m$ isomer grids by introducing other functional groups/atoms and/or linker backbone using approaches similar to those reported previously.[10,11]

Acknowledgements

The authors thank Dublin City University and the Irish Government for postgraduate funding for Mr Pavle Močilac under the PRTLI-4 T^3 initiative and Dr Neal Lemon (DCU) for managing the PRTLI-4 T^3 programme. Dr A. M. Elena and Dr J.-C. Desplat from the Irish Centre for High End Computing (ICHEC) are thanked for assistance.

References

1 W. L. Jorgensen, *Science*, 2004, **303**, 1813–1818.
2 P. G. De Benedetti and F. Fanelli, *Drug Discovery Today*, 2010, **15**, 859–866.
3 R. Guha, K. Gilbert, G. Fox, M. Pierce, D. Wild and H. Yuan, *Curr. Comput.-Aided Drug Des.*, 2010, **6**, 50–67.
4 S. Agarwal, D. Dugar and S. Sengupta, *J. Chem. Inf. Model.*, 2010, **50**, 716–731.
5 F. H. Allen, *Acta Crystallogr., Sect. B: Struct. Sci.*, 2002, **58**, 380–388.
6 T. Gelbrich, M. B. Hursthouse and T. L. Threlfall, *Acta Crystallogr., Sect. B: Struct. Sci.*, 2007, **63**, 621–632.
7 S. L. Price, M. Leslie, G. W. A. Welch, M. Habgood, L. S. Price, P. G. Karamertzanis and G. M. Day, *Phys. Chem. Chem. Phys.*, 2010, **12**, 8478–8490.
8 R. Boese, M. T. Kirchner, J. D. Dunitz, G. Filippini and A. Gavezzotti, *Helv. Chim. Acta*, 2001, **84**, 1561–1577.
9 Y. L. Slovokhotov, I. S. Neretin and J. A. K. Howard, *New J. Chem.*, 2004, **28**, 967–979.
10 P. Mocilac, M. Tallon, A. J. Lough and J. F. Gallagher, *CrystEngComm*, 2010, **12**, 3080–3090.
11 P. Mocilac, A. J. Lough and J. F. Gallagher, *CrystEngComm*, 2011, **13**, 1899–1909.
12 S. Cuffini, C. Glidewell, J. N. Low, A. G. de Oliveira, M. V. N. de Souza, T. R. A. Vasconcelos, S. M. S. V. Wardell and J. L. Wardell, *Acta Crystallogr., Sect. B: Struct. Sci.*, 2006, **62**, 651–665.
13 W. H. Ojala, J. M. Smieja, J. M. Spude, T. M. Arola, M. K. Kuspa, N. Herrera and C. R. Ojala, *Acta Crystallogr., Sect. B: Struct. Sci.*, 2007, **63**, 485–496.
14 W. H. Ojala, K. M. Lystad, T. L. Deal, J. E. Engebretson, J. M. Spude, B. Balidemaj and C. R. Ojala, *Cryst. Growth Des.*, 2009, **9**, 964–970.
15 S. I. V. Judge and C. T. Bever, *Pharmacol. Ther.*, 2006, **111**, 224–259.
16 D. T. Smith, R. Shi, R. B. Borgens, J. M. McBride, K. Jackson and S. R. Byrn, *Eur. J. Med. Chem.*, 2005, **40**, 908–917.
17 C. Ge, X. Zhang, W. Guan and Q. Liu, *J. Chem. Crystallogr.*, 2006, **36**, 459–464.
18 C. Ge, H. Kou, Z. Ni, Y. Jiang and A. Cui, *Inorg. Chim. Acta*, 2006, **359**, 541–547.
19 W. Jacob and R. Mukherjee, *Inorg. Chim. Acta*, 2006, **359**, 4565–4573.
20 J. Y. Qi, H. X. Ma, X. J. Li, Z. Y. Zhou, M. C. K. Choi, A. S. C. Chan and Q. Y. Yang, *Chem. Commun.*, 2003, 1294–1295.
21 A. Das, S. M. Peng, G. H. Lee and S. Bhattacharya, *New J. Chem.*, 2004, **28**, 712–717.
22 S. Nag, R. J. Butcher and S. Bhattacharya, *Eur. J. Inorg. Chem.*, 2007, 1251–1260.
23 M. Dasgupta, H. Tadesse, A. J. Blake and S. Bhattacharya, *J. Organomet. Chem.*, 2008, **693**, 3281–3288.
24 T. Yang, J. Y. Zhang, C. Tu, J. Lin, Q. Liu and Z. J. Guo, *Chin. J. Inorg. Chem.*, 2003, **19**, 45–48.
25 W. Jacob and R. Mukherjee, *J. Chem. Sci.*, 2008, **120**, 447–453.
26 J. Y. Qi, Y. M. Li, Z. Y. Zhou, C. M. Che, C. H. Yeung and A. S. C. Chan, *Adv. Synth. Catal.*, 2005, **347**, 45–49.
27 J. Y. Zhang, Q. Liu, C. Y. Duan, Y. Shao, J. Ding, Z. H. Miao, X. Z. You and Z. J. Guo, *J. Chem. Soc., Dalton Trans.*, 2002, 591–597.
28 *ABSFAC and CrysAlisPro CCD/RED, Version 1. 171.33.55*, Oxford Diffraction, Abingdon, Oxfordshire, UK, 2010.
29 G. M. Sheldrick, *Acta Crystallogr., Sect. A: Found. Crystallogr.*, 2008, **64**, 112–122.
30 P. McArdle, *J. Appl. Crystallogr.*, 1995, **28**, 65–65.
31 A. L. Spek, *J. Appl. Crystallogr.*, 2003, **36**, 7–13.
32 I. J. Bruno, J. C. Cole, P. R. Edgington, M. Kessler, C. F. Macrae, P. McCabe, J. Pearson and R. Taylor, *Acta Crystallogr., Sect. B: Struct. Sci.*, 2002, **58**, 389–397.
33 M. J. Frisch, G. W. Trucks, H. B. Schlegel, G. E. Scuseria, M. A. Robb, J. R. Cheeseman, G. Scalmani, V. Barone, B. Mennucci, G. A. Petersson, H. Nakatsuji, M. Caricato, X. Li, H. P. Hratchian, A. F. Izmaylov, J. Bloino, G. Zheng, J. L. Sonnenberg, M. Hada, M. Ehara, K. Toyota, R. Fukuda, J. Hasegawa, M. Ishida, T. Nakajima, Y. Honda, O. Kitao, H. Nakai, T. Vreven, J. A. Montgomery,Jr, J. E. Peralta, F. Ogliaro, M. Bearpark, J. J. Heyd, E. Brothers, K. N. Kudin, V. N. Staroverov, T. Keith, R. Kobayashi, J. Normand, K. Raghavachari, A. Rendell, J. C. Burant, S. S. Iyengar, J. Tomasi, M. Cossi, N. Rega, J. M. Millam, M. Klene, J. E. Knox, J. B. Cross, V. Bakken, C. Adamo, J. Jaramillo, R. Gomperts, R. E. Stratmann, O. Yazyev, A. J. Austin, R. Cammi, C. Pomelli, J. W. Ochterski, R. L. Martin, K. Morokuma, V. G. Zakrzewski, G. A. Voth, P. Salvador, J. J. Dannenberg, S. Dapprich, A. D. Daniels, O. Farkas, J. B. Foresman, J. V. Ortiz, J. Cioslowski and D. J. Fox, *Gaussian 09, Revision B. 01*, Gaussian, Inc., Wallingford, CT, 2010.
34 A. V. Marenich, C. J. Cramer and D. G. Truhlar, *J. Phys. Chem. B*, 2009, **113**, 6378–6396.
35 J. A. Montgomery, J. W. Ochterski and G. A. Petersson, *J. Chem. Phys.*, 1994, **101**, 5900–5909.
36 H. V. R. Dias and T. K. H. H. Goh, *Polyhedron*, 2004, **23**, 273–282.
37 S. A. Barnett, A. T. Hulme and D. A. Tocher, *Acta Crystallogr., Sect. C: Cryst. Struct. Commun.*, 2006, **62**, o412–o415.
38 F. G. Vogt, J. A. Vena, M. Chavda, J. S. Clawson, M. Strohmeier and M. E. Barnett, *J. Mol. Struct.*, 2009, **932**, 16–30.
39 J. McMahon, J. F. Gallagher, F. P. Anderson and A. J. Lough, *Acta Crystallogr., Sect. C: Cryst. Struct. Commun.*, 2009, **65**, o345–o351.
40 D. Percival, J. M. D. Storey and W. T. A. Harrison, *Acta Crystallogr., Sect. E: Struct. Rep. Online*, 2007, **63**, o1851–o1852.
41 B. T. Gowda, B. P. Sowmya, J. Kozisek, M. Tokarcik and H. Fuess, *Acta Crystallogr., Sect. E: Struct. Rep. Online*, 2007, **63**, o2906.

 This journal is © The Royal Society of Chemistry 2011